Z. Phys. C – Particles and Fields 46, 1–7 (1990)

Zeitschrift für Physik C Particles and Fields

A study of photon production in hadronic events from e^+e^- annihilation

JADE Collaboration

D.D. Pitzl[2,a], J. Allison[5], K. Ambrus[3,b], R.J. Barlow[5], W. Bartel[1], S. Bethke[3], C.K. Bowdery[4], S.L. Cartwright[7,c], J. Chrin[5], D. Clarke[7], A. Dieckmann[3], I.P. Duerdoth[5], G. Eckerlin[3], E. Elsen[3], R. Felst[1], A.J. Finch[4], F. Foster[4], T. Greenshaw[2], J. Hagemann[2,l], D. Haidt[1], J. Heintze[3], G. Heinzelmann[2], K.H. Hellenbrand[3,d], P. Hill[6,k], G. Hughes[4], H. Kado[1,e], K. Kawagoe[8], C. Kleinwort[2,l], G. Knies[1], T. Kobayashi[8], S. Komamiya[3,f], H. Krehbiel[1], J. v. Krogh[3], M. Kuhlen[2,g], F.K. Loebinger[5], A.A. Macbeth[5], N. Magnussen[1,h], R. Marshall[7], R. Meinke[1], R.P. Middleton[7], H. Minowa[8], P.G. Murphy[5], B. Naroska[1], J.M. Nye[4], J. Olsson[1], F. Ould-Saada[2], R. Ramcke[1], H. Rieseberg[3], D. Schmidt[1,h], L. Smolik[3], U. Schneekloth[2,m], J.A.J. Skard[6,i], J. Spitzer[3,j], P. Steffen[1], K. Stephens[5], A. Wagner[3], I.W. Walker[4], G. Weber[2], M. Zimmer[3], G.T. Zorn[6]

[1] Deutsches Elektronen-Synchrotron DESY, Hamburg, Federal Republic of Germany
[2] II. Institut für Experimentalphysik der Universität Hamburg, Hamburg, Federal Republic of Germany
[3] Physikalisches Institut der Universität Heidelberg, Heidelberg, Federal Republic of Germany
[4] University of Lancaster, Lancaster, England
[5] University of Manchester, Manchester, England
[6] University of Maryland, College Park, MD, USA
[7] Rutherford Appleton Laboratory, Chilton, Didcot, England
[8] International Center for Elementary Particle Physics, University of Tokyo, Tokyo, Japan

Received 16 October 1989

Abstract. Results are presented on an investigation of photons produced in multihadronic final states from e^+e^- annihilation at 35 GeV and 44 GeV center of mass energies. Scaling violation between 14 and 44 GeV is observed in inclusive photon spectra. Comparing inclusive π^0 spectra with charged pion spectra it is found that the average π^0 multiplicity exceeds the charged pion multiplicity scaled by factor of 0.5 by $(16\pm5)\%$ and $(21\pm7)\%$ at 35 and 44 GeV respectively. The excess can be attributed to isospin violating decays of hadrons. The η multiplicity is found to be $\langle n_\eta\rangle = 0.64\pm0.09\pm0.06$ at 35 GeV. With a significance of three standard deviations a signal from quark bremsstrahlung is observed. The measured charge asymmetry in hadronic final states, due to the interference between initial and final state radiation, of $A=-0.141\pm0.041$ is in accord with QED expectations. An interference effect in the azimuth angle distribution of charged jets around the photon direction is observed for the first time.

[a] Now at Santa Cruz, Cal., USA
[b] Now at MBB, München, FRG
[c] Now at Sheffield University, UK
[d] Now at Universität des Saarlandes, Saarbrücken, FRG
[e] Now at Bayer Ag, Brunsbüttel, FRG
[f] Now at SLAC, Cal., USA
[g] Now at CALTECH, Cal., USA
[h] Universität-Gesamthochschule Wuppertal, Wuppertal, FRG
[i] Now at ST Systems Corporation, Lanham, MD, USA
[j] Now at MPI, Heidelberg, FRG
[k] Now at DESY, Hamburg, FRG
[l] Now at CERN, Geneva, Switzerland
[m] Now at MIT, Boston, USA

Introduction

Photons in hadronic events from e^+e^- annihilation may be associated with two different types of processes. They can be decay products of mesons and baryons or be emitted as bremsstrahlung photons by the incoming leptons or final state quarks. The latter are called direct photons and a study of their properties may be used to test the current picture of hadron production in which fractionally charged quarks are created in e^+e^- annihilation and then fragment into hadrons [1]. The majority of the observed photons are of hadronic origin and stem from π^0 and η decays. A reconstruction of the parent particles allows a comparison with the inclusive spectra of charged pions and kaons.

In a previous investigation the JADE collaboration has studied the production of photons at lower energy [2]. The present analysis is based on a high energy data sample taken with the JADE detector at PETRA corresponding to an integrated luminosity of 176 pb^{-1} at an

average center of mass energy of $\sqrt{s}=34.9$ GeV and 43 pb^{-1} at 43.8 GeV.

Photons are recorded in the JADE detector by a fine grained array of lead glass counters [3] with angular coverage up to $|\cos\Theta|\leqq 0.98$. Compared with the set – up used in the previous analysis the photon detection system has been improved by replacing some of the central lead glass blocks (SF5) with a depth of 12 radiation lengths by material with a shorter radiation length (SF6) thus increasing the depth to 18 radiation lengths. This means that the energy resolution could be maintained at $\sigma(E_\gamma)/E_\gamma=0.04/\sqrt{E_\gamma(\mathrm{GeV})}+0.015$ between 6 GeV and the highest photon energy of 22.5 GeV. The method of reconstructing photons by a fit of shower profiles to neutral lead glass clusters is unchanged with respect to the procedure followed in [2]. The angular resolution, $\sigma_\Theta=12$ mrad, and $\sigma_\Phi=10$ mrad for photons coming from the interaction point, also remained the same. For this analysis only photons in the so called barrel region $|\cos\Theta|\leqq 0.76$ were considered.

Inclusive photon spectra

The inclusive photon spectra at the two energies, corrected for initial state radiation, are shown in Fig. 1 together with previous JADE results at lower center of mass energies [2]. A small scaling violation effect is observed when the inclusive cross sections at 14 and 44 GeV are compared. A quantitative measure for this effect is obtained by integrating the spectra in the interval $0.2<x<0.4$, where x is the normalised photon energy $x=E_\gamma/E_{\mathrm{beam}}$. The ratio of the integrals $I(14\ \mathrm{GeV})/I(44\ \mathrm{GeV})=1.6\pm0.3$, where $I(\sqrt{s})=\int_{0.2}^{0.4} s\frac{d\sigma}{dx}dx$. This can be compared with the Lund model [4] expectation of 1.20 for this ratio. QCD based models attribute scale violating effects to an increase of gluon emission with increasing energy.

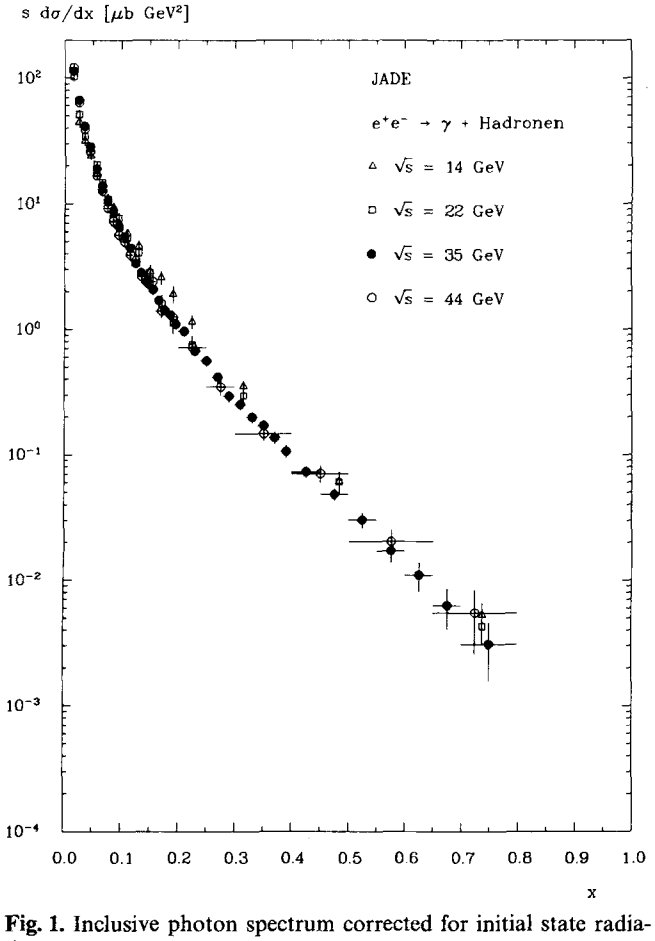

Fig. 1. Inclusive photon spectrum corrected for initial state radiation

The photon multiplicities $\langle n_\gamma\rangle=\frac{1}{\sigma_{\mathrm{tot}}}\int_{x_{\min}}^{1}\frac{d\sigma}{dx}dx$ are computed by integrating the measured inclusive spectra and correcting for the unobserved x range by extrapolating to $x=0$ with a slope as predicted by the Lund model. The results are summarized in Table 1 in which the first and second errors are statistical and systematic respectively.

The energy fractions ρ_γ carried by photons are computed by integrating the measured spectra weighted with the normalized photon energy x: $\langle\rho_\gamma\rangle=\frac{1}{\sigma_{\mathrm{tot}}}\int_{x_{\min}}^{1}x\cdot\frac{d\sigma}{dx}dx$. As shown in Table 2 photons carry about one quarter of the total center of mass energy.

Inclusive π^0 and η spectra

The majority of photons observed in hadronic events can be associated with π^0 decays. The inclusive π^0 spectra are obtained by evaluating the π^0 contribution to the two photon invariant mass spectra, which show a clear signal centered at 135 MeV having a width of $\sigma=17.2$ MeV, as indicated in Fig. 2a for $\sqrt{s}=35$ GeV.

Table 1. The number of photons per event with fractional energies above $x_{\min}$

$\langle n_\gamma\rangle$		
$\sqrt{s}$	$x_{\min}=0.01$	$x_{\min}=0.0$
35 GeV	$10.0\pm0.05\pm0.5$	$14.3\pm0.07\pm0.7$
44 GeV	$9.9\pm0.09\pm0.5$	$15.4\pm0.14\pm0.8$

Table 2. The fraction of cms energy carried by photons with fractional energies above $x_{\min}$

ρ_γ		
$\sqrt{s}$	$x_{\min}=0.01$	$x_{\min}=0.0$
35 GeV	$0.243\pm0.008\pm0.017$	$0.253\pm0.009\pm0.018$
44 GeV	$0.223\pm0.012\pm0.016$	$0.237\pm0.013\pm0.017$

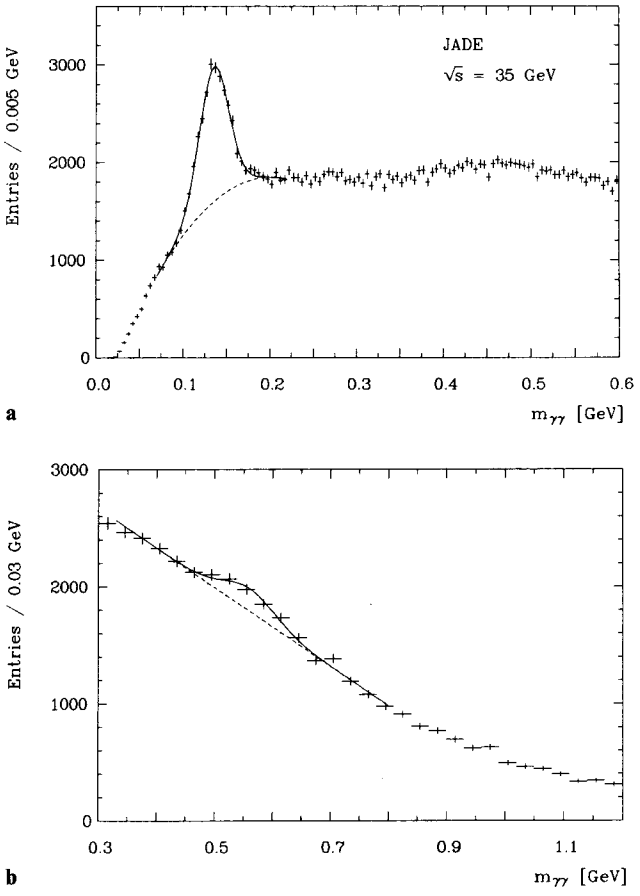

Fig. 2. a Two photon invariant mass spectrum with a Gaussian fit to the π^0 signal (mass $m=135.4\pm0.5$ MeV, width $\sigma=17.2\pm0.6$ MeV) and a second order polynomial fit to the combinatorial background. **b** Two photon invariant mass spectrum after the cuts described in the text with a Gaussian fit to the η signal (mass $m=556\pm8$ MeV, width $\sigma=45\pm9$ MeV) and a straight line fit to the combinatorial background

In order to keep the combinatorial background at a reasonable level, only photons with an energy above $E_\gamma = 200$ MeV have been considered. In Fig. 3a and b the inclusive cross sections for π^0 production are shown as a function of the normalised pion energy for both center of mass energies. The corresponding π^0 multiplicities, shown in Table 3, are calculated by integrating the measured spectra and using the Lund model to extrapolate into the region which is not accessible to the experiment.

It is observed that the neutral pion spectra lie systematically above the charged pion spectra measured by TASSO [5] after these have been scaled by a factor 1/2. In the momentum range where both neutral and charged pions can be observed the ratio of their spectra is mea-

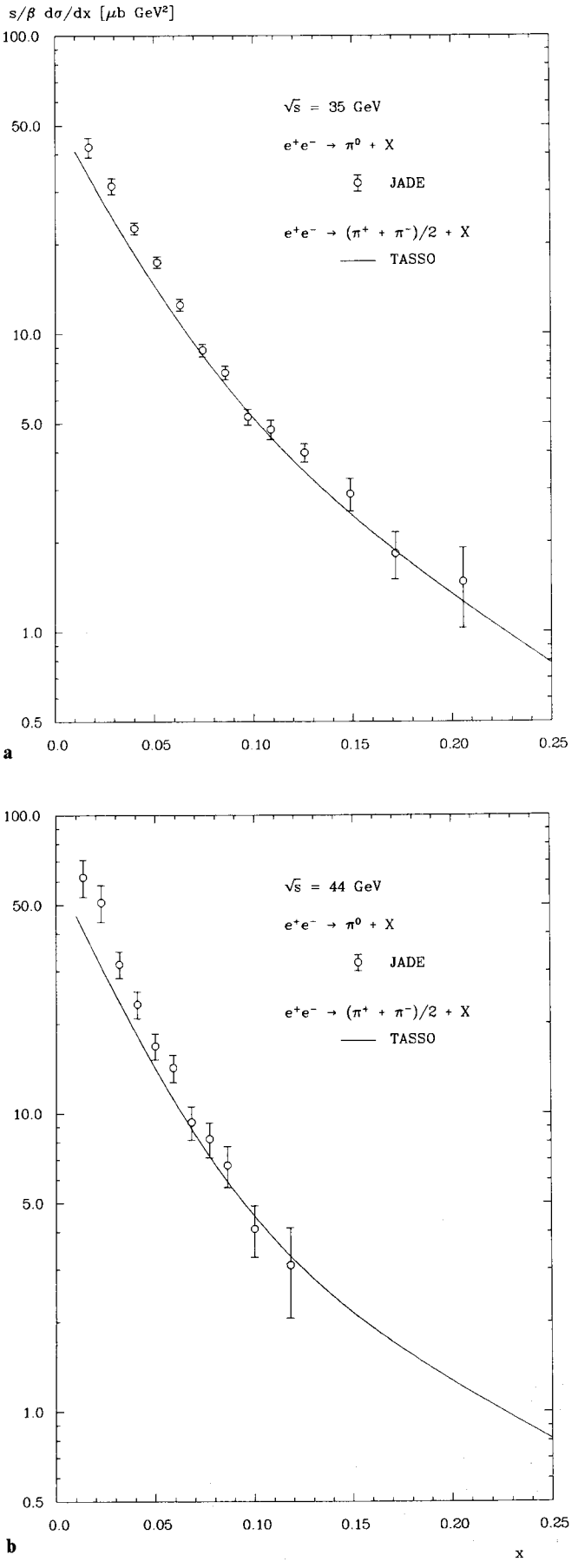

Fig. 3. a Inclusive π^0 spectrum at $\sqrt{s}=35$ GeV shown with a fit to the TASSO [5] charged pion spectrum scaled by 1/2. **b** Inclusive π^0 spectrum at $\sqrt{s}=44$ GeV shown with a fit to the TASSO charged pion spectrum scaled by 1/2

Table 3. π^0 multiplicities

$\sqrt{s}$	$\langle n_{\pi^0} \rangle$
35 GeV	$6.4 \pm 0.1 \pm 0.4$
44 GeV	$7.0 \pm 0.25 \pm 0.45$

sured to be:

$$\sqrt{s}=35 \text{ GeV}: \frac{2\frac{d\sigma}{dx}(\pi^0)}{\frac{d\sigma}{dx}(\pi^+)+\frac{d\sigma}{dx}(\pi^-)} = 1.16 \pm 0.05$$

for $x<0.2$

$$\sqrt{s}=44 \text{ GeV}: \frac{2\frac{d\sigma}{dx}(\pi^0)}{\frac{d\sigma}{dx}(\pi^+)+\frac{d\sigma}{dx}(\pi^-)} = 1.21 \pm 0.07$$

for $x<0.12$.

The Lund model predicts a higher π^0 rate and attributes it to isospin violating decays such as $\eta \to 3\pi^0$ or $\omega \to \gamma\pi^0$.

The restricted x range accessible and the limited accuracy of the measured π^0 spectra make it impossible to observe the scale violating effects predicted by first order QCD.

After removing all photons which contribute to the π^0 signal in the two photon mass spectrum at $\sqrt{s}=35$ GeV and introducing additional cuts on the photon quality, a signal is observed at the location of the η meson, that is at $m_{\gamma\gamma}=(556 \pm 8)$ MeV with a width of $\sigma=(45 \pm 9)$ MeV. The two photon mass spectrum, after cuts, is shown in Fig. 2b. The η multiplicity extrapolated over the entire kinematic range is $n_\eta = 0.64 \pm 0.09 \pm 0.06$ in agreement with an earlier JADE result [3]. The inclusive cross section for η production is shown in Fig. 4.

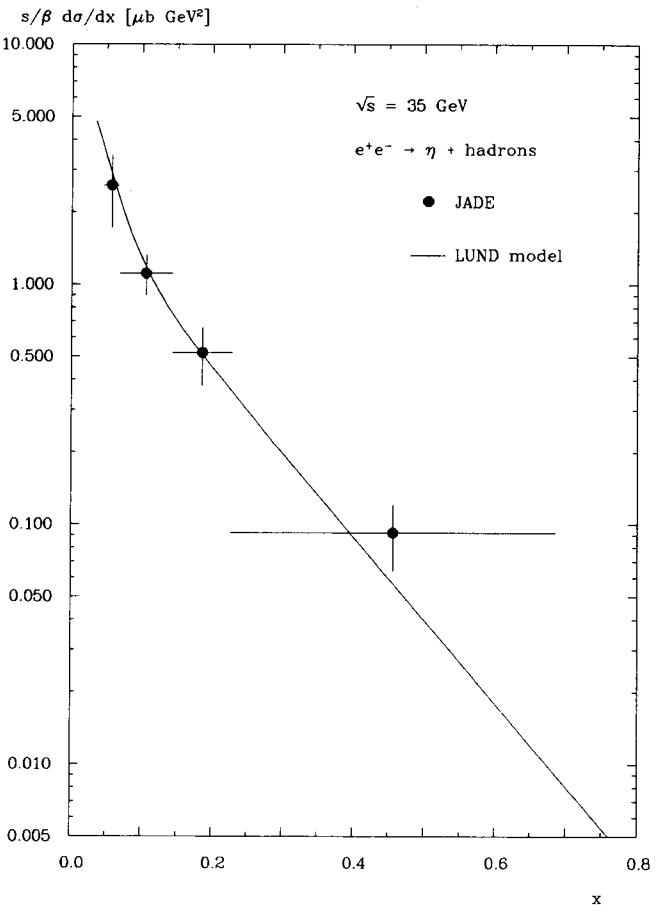

Fig. 4. Inclusive η spectrum at $\sqrt{s}=35$ GeV shown with the Lund model prediction

Quark bremsstrahlung

A search was made for bremsstrahlung photons emitted by the primary quarks at $\sqrt{s}=35$ GeV. In order to suppress the background, mainly due to photons coming from π^0 decays, the following criteria were applied:

- The normalised photon energy was required to be in the range $0.2<x<0.8$.
- The photons had to be isolated, that is the summed charged and neutral energy in a cone with half opening angle of 30° around the photon direction was required to be less than 0.5 GeV.
- Two jet axes were reconstructed in each event. First a Lorentz transformation into the hadronic rest system was performed with the photon direction as boost axis and the sphericity axis was determined. The hadrons were then transformed back into the lab system resulting in an event with two jet axes. The transverse momentum of the hard photon was measured with respect to these axes and only those photons having transverse momenta larger than 3 GeV were accepted.

A total of 723 photons fulfill these criteria including 9 events with two isolated hard photons.

The observed spectrum is compared to Monte Carlo calculations made using a program by Berends et al. [6] which simulates e^+e^- annihilation into quark pairs and includes all QED effects up to order α^3. Fractional quark charges and constituent quark masses are used in the calculations, while quark fragmentation was simulated according to the Lund scheme. QCD corrections, which take into account that bremsstrahlung photons may also be emitted from inside the parton cascade in the fragmentation process, are expected to be much smaller than 25% [8] in the present analysis, mainly due to the stringent isolation cuts for the energetic photon. The corrections have been neglected.

Evidence for the presence of quark bremsstrahlung is obtained by comparing the data to computations with and without quark bremsstrahlung. As demonstrated in Fig. 5 the agreement between the observed and the computed spectra is better when quark bremsstrahlung is

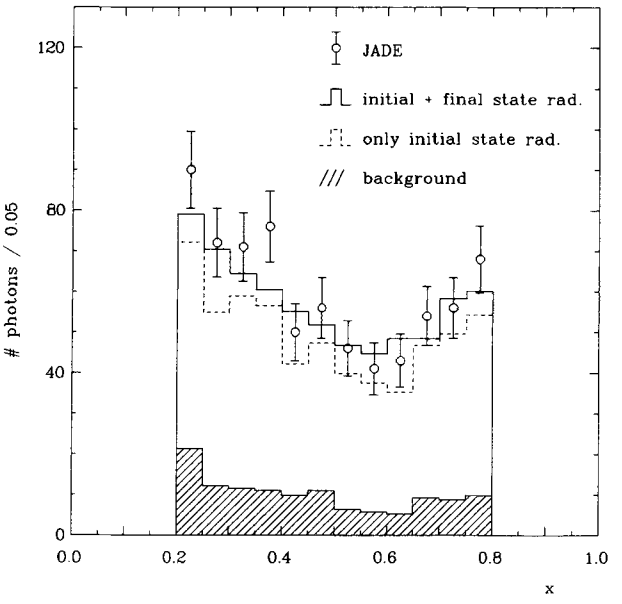

Fig. 5. Observed direct photon spectrum shown with the spectra from the Monte Carlo simulations with and without final state radiation

included in the calculations, and the difference between the expected number of photons including final state bremsstrahlung and the observed number is 38 ± 40. The number of photons which can be attributed to quark bremsstrahlung is 128 ± 41. The 9 events with two isolated photons are probably due to the fourth order QED process $e^+e^- \to q\bar{q}\gamma\gamma$. Of the remaining photons about 21% are background from hadron decays and 79% from initial state radiation.

The presence of quark bremsstrahlung is corroborated by the observation of a charge asymmetry of the final state jets with respect to the incident positron direction. The origin of this asymmetry is due to the interference of two amplitudes with opposite charge conjugation quantum numbers which contribute to the process $e^+e^- \to q\bar{q}\gamma$. The final state $q\bar{q}$ system has $C=-1$ if the photon is radiated by the incoming leptons and $C=+1$ if the final state quarks radiate. In order to determine the asymmetry experimentally, quark directions are approximated by a corresponding jet axis, while the sign of the quark charge is inferred from the jet charges w.

The jet axes are determined in the rest system of the final state hadrons, which is related to the laboratory system through a Lorentz boost in the direction of the bremsstrahlung photon. In this system two back to back jets fix the sphericity axis and the corresponding jet directions in the laboratory system are obtained by reversing the Lorentz boost. Jet charges w are calculated by summing all charges in one jet weighted by the longitudinal particle momenta with respect to the sphericity axis:

$$w = \sum_i q_i \left(\frac{p_i^L}{p_{\text{jet}}^L} \right)^{\alpha}.$$

The jet with the larger value w in one event is taken to be positively charged. The value of α is optimised to measure quark charges. With the choice $\alpha = 0.5$ the sign of the quark charge associated with a particular jet is correctly reproduced in 69% of the cases according to Monte Carlo calculations based on the Lund model. Only events where both jets contain at least two charged particles and both jet axes have $|\cos\Theta_{\text{jet}}| < 0.90$ are kept. The latter requirement reduces charge determination difficulties connected with particle losses in the beam pipe.

The angular distribution of the positively charged jet with respect to the beam axis is shown in Fig. 6. An asymmetry of $A = -0.141 \pm 0.041$ is observed, which agrees well with the asymmetry of $A_{\text{MC}} = -0.122 \pm 0.014$ predicted by QED from the interference of initial and final state radiation and including detector effects.

The charge asymmetry in the polar angle distribution has been seen also by other experiments [9]. Another manifestation of interference phenomena is, however, observed for the first time in the azimuth angle distribution of positively charged jets around the photon direction, which was predicted by Cudell, Halzen and Herzog [7]. The azimuth angle Φ is measured between the incident positron direction and the axis of the positively charged jet in the plane perpendicular to the photon direction (see Fig. 7). The measured azimuth angle distribution is shown in Fig. 8 together with two Monte Carlo simulations with and without final state radiation. Due to the

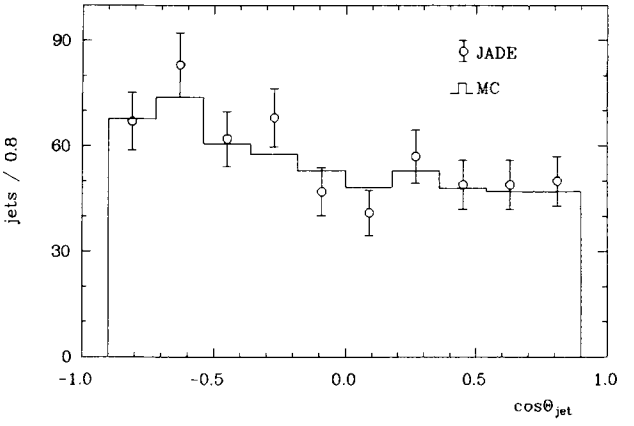

Fig. 6. Angular distribution of positively charged jets. The angle Θ_{jet} is measured between the jet axis and the incident positron direction

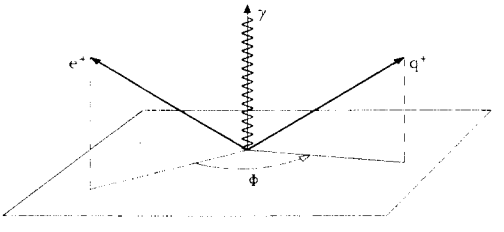

Fig. 7. Definition of the azimuth angle Φ

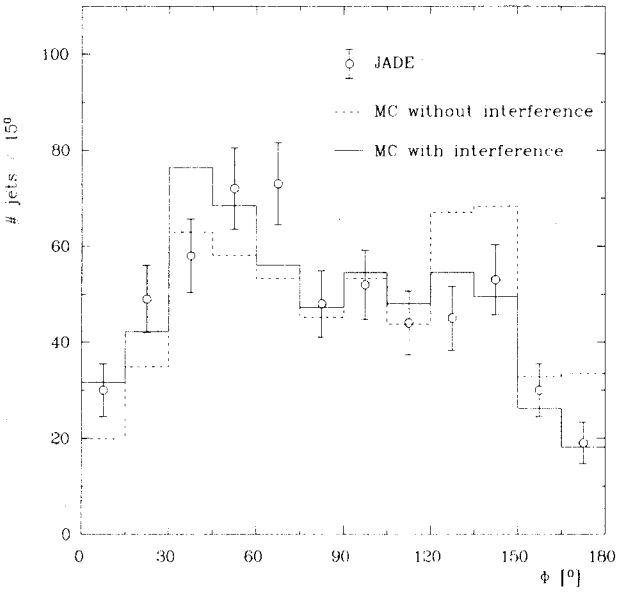

Fig. 8. Measured Φ distribution of the positively charged jets shown with the distributions from the Monte Carlo simulations with and without interference of initial and final state radiation

cuts on the photon and jet polar angles the Φ distribution is not flat when the interference effect is neglected in the simulation. An acceptable description of the measured distribution is obtained only when the interference is taken into account in the simulation. The χ^2 values and the corresponding χ^2 probabilities P for the two simulations with respect to the data are:

with interference: $\chi^2 = 12.1$ for 11 degrees of freedom, $P = 0.36$

without interference: $\chi^2 = 23.6$ for 11 degrees of freedom, $P = 0.015$.

The measured asymmetries confirm the assumption that final state bremsstrahlung has been observed with a cross section which is expected for a process where pointlike charged constituents are primarily produced in an e^+e^- annihilation process. Although the data presented agree with calculations of final state bremsstrahlung effects assuming fractionally charged quarks, these measurements do not exlude all models with integrally charged quarks [10].

Acknowledgements. We are indebted to the PETRA machine group and the DESY computer center staff for their excellent support during the experiment and to the engineers and technicians of the collaborating institutions who have participated in the construction and maintenance of the apparatus. This experiment was supported by the Bundesministerium für Forschung und Technologie, by the Ministry of Education, Science and Culture of Japan, by the UK Science and Engineering Research Council, through the Rutherford Appleton Laboratory and by the US Department of Energy. The visiting groups wish to thank the Desy Directorate for the hospitality extended to them.

Appendix

Table 4. Inclusive photon spectrum at $\sqrt{s} = 35$ GeV

x	$\langle x \rangle$	$s\,d\sigma/dx \pm$stat.	$\pm$syst. [μb GeV^2]
0.01–0.02	0.015	138.8 ±0.41	±7.6
0.02–0.03	0.025	66.4 ±0.32	±4.4
0.03–0.04	0.035	41.2 ±0.27	±2.3
0.04–0.05	0.045	28.4 ±0.24	±1.3
0.05–0.06	0.055	18.9 ±0.20	±0.85
0.06–0.07	0.065	13.8 ±0.17	±0.62
0.07–0.08	0.075	10.4 ±0.16	±0.47
0.08–0.09	0.085	8.61 ±0.15	±0.39
0.09–0.10	0.095	6.60 ±0.13	±0.43
0.10–0.11	0.105	5.49 ±0.12	±0.44
0.11–0.12	0.115	4.47 ±0.11	±0.36
0.12–0.13	0.125	3.33 ±0.097	±0.27
0.13–0.14	0.135	2.82 ±0.090	±0.23
0.14–0.15	0.145	2.33 ±0.081	±0.19
0.15–0.16	0.155	2.07 ±0.076	±0.17
0.16–0.17	0.165	1.70 ±0.068	±0.14
0.17–0.18	0.175	1.43 ±0.061	±0.11
0.18–0.19	0.185	1.31 ±0.059	±0.10
0.19–0.20	0.195	1.10 ±0.054	±0.09
0.20–0.22	0.21	0.967 ±0.037	±0.08
0.22–0.24	0.23	0.673 ±0.029	±0.05
0.24–0.26	0.25	0.564 ±0.028	±0.045
0.26–0.28	0.27	0.418 ±0.022	±0.033
0.28–0.30	0.29	0.295 ±0.018	±0.024
0.30–0.32	0.31	0.253 ±0.016	±0.020
0.32–0.34	0.33	0.200 ±0.014	±0.016
0.34–0.36	0.35	0.171 ±0.012	±0.014
0.36–0.38	0.37	0.137 ±0.010	±0.011
0.38–0.40	0.39	0.107 ±0.008	±0.009
0.40–0.45	0.425	0.0732 ±0.0047	±0.0060
0.45–0.50	0.475	0.0486 ±0.0032	±0.0040
0.50–0.55	0.525	0.0305 ±0.0022	±0.0035
0.55–0.60	0.575	0.017 ±0.0014	±0.0030
0.60–0.65	0.625	0.011 ±0.0010	±0.0029
0.65–0.70	0.675	0.0063 ±0.00047	±0.0022
0.70–0.80	0.75	0.0031 ±0.00019	±0.0015

Table 5. Inclusive photon spectrum at $\sqrt{s} = 44$ GeV

x	$\langle x \rangle$	$s\,d\sigma/dx \pm$stat.	$\pm$syst. [μb GeV^2]
0.01–0.02	0.015	121.3 ±1.1	±8.8
0.02–0.03	0.025	63.6 ±0.82	±4.6
0.03–0.04	0.035	38.9 ±0.70	±2.8
0.04–0.05	0.045	25.9 ±0.61	±1.9
0.05–0.06	0.055	16.8 ±0.50	±1.2
0.06–0.07	0.065	12.6 ±0.46	±0.92
0.07–0.08	0.075	9.23 ±0.41	±0.72
0.08–0.09	0.085	7.25 ±0.37	±0.58
0.09–0.10	0.095	5.64 ±0.34	±0.45
0.10–0.11	0.105	4.99 ±0.32	±0.40
0.11–0.12	0.115	3.91 ±0.29	±0.31
0.12–0.13	0.125	3.53 ±0.28	±0.28
0.13–0.14	0.135	2.63 ±0.24	±0.21
0.14–0.15	0.145	2.42 ±0.24	±0.19
0.15–0.16	0.155	2.40 ±0.23	±0.19
0.16–0.18	0.17	1.40 ±0.13	±0.11
0.18–0.20	0.19	1.25 ±0.12	±0.10
0.20–0.25	0.225	0.718 ±0.056	±0.057
0.25–0.30	0.275	0.349 ±0.038	±0.028
0.30–0.40	0.35	0.147 ±0.015	±0.011
0.40–0.50	0.45	0.071 ±0.0087	±0.0067
0.50–0.65	0.575	0.021 ±0.0025	±0.0042
0.65–0.80	0.725	0.0055 ±0.00079	±0.0028

Table 6. Inclusive π^0 spectrum at $\sqrt{s}=35$ GeV

E_{π^0}[GeV]	<x>	$s/\beta \cdot d\sigma/dx \pm$stat. $\pm$syst. [μb GeV^2]
0.2–0.4	0.0171	42.3 ± 1.9 ± 3.1
0.4–0.6	0.0286	31.3 ± 1.3 ± 1.7
0.6–0.8	0.0400	22.6 ± 0.62 ± 1.0
0.8–1.0	0.0514	17.4 ± 0.45 ± 0.61
1.0–1.2	0.0629	12.5 ± 0.35 ± 0.45
1.2–1.4	0.0743	8.76 ± 0.30 ± 0.30
1.4–1.6	0.0857	7.39 ± 0.24 ± 0.27
1.6–1.8	0.0971	5.26 ± 0.22 ± 0.23
1.8–2.0	0.109	4.77 ± 0.24 ± 0.22
2.0–2.4	0.126	3.99 ± 0.18 ± 0.21
2.4–2.8	0.149	2.90 ± 0.27 ± 0.24
2.8–3.2	0.171	1.83 ± 0.24 ± 0.25
3.2–4.0	0.206	1.47 ± 0.27 ± 0.28

Table 7. Inclusive π^0 spectrum at $\sqrt{s}=44$ GeV

E_{π^0} [GeV]	$\langle x \rangle$	stat. $\pm$syst. [μb GeV^2]
0.2–0.4	0.0136	62.2 $\pm 5.8 \pm 6.6$
0.4–0.6	0.0227	50.7 $\pm 3.6 \pm 4.6$
0.6–0.8	0.0318	31.6 $\pm 2.1 \pm 2.4$
0.8–1.0	0.0409	23.2 $\pm 1.6 \pm 1.8$
1.0–1.2	0.0500	16.8 $\pm 1.2 \pm 1.2$
1.2–1.4	0.0591	14.2 $\pm 1.0 \pm 1.1$
1.4–1.6	0.0682	9.34 $\pm 1.0 \pm 0.9$
1.6–1.8	0.0773	8.2 $\pm 0.9 \pm 0.8$
1.8–2.0	0.0864	6.7 $\pm 1.0 \pm 0.8$
2.0–2.4	0.100	4.1 $\pm 0.6 \pm 0.6$
2.4–2.8	0.118	3.1 $\pm 0.8 \pm 0.9$

Table 8. Inclusive η spectrum at $\sqrt{s}=35$ GeV

E_η [GeV]	$\langle x \rangle$	stat. $\pm$syst. [μb GeV^2]
0.8– 1.2	0.057	2.6 ± 0.9 ± 0.8
1.2– 2.5	0.106	1.1 ± 0.19 ± 0.13
2.5– 4.0	0.186	0.52 $\pm 0.094 \pm 0.08$
4.0–12.0	0.457	0.092 $\pm 0.025 \pm 0.015$

Table 9. Cross section for the process $e^+e^- \to q\bar{q}\gamma$ with $|\cos\Theta_\gamma| < 0.76$ at $\sqrt{s}=35$ GeV

x	$\langle x \rangle$	$d\sigma/dx \pm$stat. $\pm$syst. [pb]
0.2–0.3	0.25	17.9 ± 1.6 ± 1.4
0.3–0.4	0.35	13.3 ± 1.2 ± 1.1
0.4–0.5	0.45	8.9 ± 1.0 ± 0.7
0.5–0.6	0.55	7.4 $\pm 0.85 \pm 0.6$
0.6–0.7	0.65	6.9 $\pm 0.76 \pm 0.6$
0.7–0.8	0.75	7.3 $\pm 0.71 \pm 0.6$

References

1. T.F. Walsh, P. Zerwas: Phys. Lett. 44 B (1973) 195
2. JADE-Coll., W. Bartel et al.: Z. Phys. C – Particles and Fields 28 (1985) 343
3. JADE-Coll., W. Bartel et al.: Phys. Lett. 88 B (1979) 171
4. T. Sjöstrand: Comp. Phys. Commun. 27 (1982) 243; T. Sjöstrand: Comp. Phys. Commun. 28 (1983) 229; T. Sjöstrand, M. Bengtsson: Comp. Phys. Commun. 43 (1987) 367
5. TASSO-Coll., W. Braunschweig et al.: Z. Phys. C – Particles and Fields 42 (1989) 189
6. F.A. Berends, R. Kleiss, S. Jadach: Nucl. Phys. B202 (1982) 63; F.A. Berends, R. Kleiss, S. Jadach: Comp. Phys. Commun. 29 (1983) 185
7. J.R. Cudell, F. Halzen, F. Herzog: Phys. Lett. 140 B (1984) 83
8. E. Laerman, T.F. Walsh, I. Schmitt, P.M. Zerwas: Nucl. Phys. B207 (1982) 205
9. MAC-Coll., E. Fernandez et al.: Phys. Rev. Lett. 54 (1985) 95; MARK II-Coll., M.S. Gold: Ph.D. Thesis LBL-22433; TASSO-Coll., W. Braunschweig et al.: Z. Phys. C – Particles and Fields 1 (1988) 385
10. H.J. Lipkin: Phys. Lett. 85 B (1979) 236; T. Jayaraman, G. Rajasekaran, S.D. Rindani: Phys. Rev. D32 (1985) 1262; X.-G. He, S. Pakvasa, G. Rajasekaran, S.D. Rindani: Phys. Lett. B185 (1987) 158